IL NUOVO CIMENTO Vol. 5 C, N. 4 Luglio-Agosto 1982

Grain Growth in Ice.

L. Levi (*) and E. A. Ceppi (**)

IFA, Servicio Meteorológico Nacional - Buenos Aires, Argentina
IMAF, Universidad Nacional de Córdoba - Córdoba, Argentina

(ricevuto il 19 Agosto 1982)

Summary. — Grain growth is studied in polycrystalline ice, consisting of elongated grains, of $(200 \div 300)$ μm mean width $\bar{w}$ and $(2 \div 3)$ mm mean length $\bar{l}$. The samples are annealed at different temperatures, between 0 °C and — 10 °C. It is found that $\bar{l}$ is not affected by annealing, while $\bar{w}$ increases with the annealing time. Below the melting point, $\bar{w}(t)$ tends to a limit value $\bar{w}_s$. This behaviour is related to the pinning action of air bubbles, which would be similar to that found for solid inclusions in metals. By assuming $\bar{w}_s = \bar{d}/f$, where $\bar{d}$ is the mean bubble diameter and f is the volume fraction of air dissolved in water, reasonable values are found for $\bar{d}$. The activation energy of the phenomenon is evaluated on the basis of the present and of Jellinek and Gouda's results. It is found $Q = 0.6$ eV, which value approximately coincides with that for bulk self-diffusion as it occurs for metals, several degrees below the melting point. This coincidence suggests that, for ice, grain growth would be controlled by bulk impurity diffusion up to the very melting point.

PACS. 92.60. – Meteorology.

1. – Introduction.

Polycrystalline ice is abundant in nature. When natural ice samples are studied, it must be taken into account that their initial structure may get

(*) Comisión Nacional de Energía Atómica, Fellow of the Consejo Nacional de Investigaciones Científicas y Técnicas (CONICET).
(**) Instituto de Matemática, Astronomía y Física, Universidad Nacional de Córdoba and CONICET.

modified during the time elapsed after their formation. Among the structural changes that take place in the solid, grain growth, occurring under the action of the grain boundary surface free energy, may be important, especially at temperatures near the melting point. Since these temperatures usually prevail in the surroundings of natural ice and in cold rooms where the samples are stored before the analysis, information about this process is of interest.

The most extensive work on grain growth in ice crystals has been performed by JELLINEK and GOUDA [1]. These authors studied the phenomenon at different annealing temperatures from -2 °C to -30 °C and represented their results by applying the well-known expression

$$b = k_n t^n , \tag{1}$$

with

$$k_n = k_{n0} \exp [- Q_n/kT] , \tag{1'}$$

where b is the mean crystal diameter, t the annealing time, n a constant exponent and k_n a rate parameter; this depends on the temperature T through the activation energy Q_n, according to Arrhenius equation (1').

As shown by the theory [2-4], for an ideal grain growth process n should be equal to 0.5, though the value of this exponent has been frequently found to be smaller. Using as samples to be analysed thin ice sheets grown by rapid freezing of double distilled water extended on microscope slides, JELLINEK and GOUDA [1] obtained for the parameters in (1) and (1')

$$n = 0.3 , \quad k_{n0} = 1.56 \cdot 10^3 \text{ cm/d}^n , \quad Q_n = 5600 \text{ cal/mol} .$$

Other researchers [5-8] were mainly interested in obtaining information about the structural changes that could have occurred in hailstones after having suffered some degree of annealing. Actually, grain growth occurring before collection and during storage should be taken into account when measurements of the crystal size are performed to derive the corresponding hailstone growth conditions. In the mentioned works, samples with very different initial structures, most of which prepared from natural hailstones and from ice grown in

---

(1) H. H. G. JELLINEK and V. K. GOUDA: *Phys. Status Solidi*, **31**, 413 (1969).
(2) P. FELTHAM: *Acta Metall.*, **5**, 97 (1957).
(3) N. P. LOUAT: *Acta Metall.*, **27**, 721 (1974).
(4) M. HILLERT: *Acta Metall.*, **13**, 227 (1965).
(5) A. E. CARTE: *Bull. Ob. Puy de Dome*, 2ème ser. (1961), p. 846.
(6) D. S. ROOS: *J. Glaeiol.*, **6**, 411 (1966).
(7) C. A. KNIGHT, T. ASHWORTH and N. C. KNIGHT: *J. Atmos. Sci.*, **35**, 1997 (1978).
(8) F. PRODI and L. LEVI: *J. Atmos. Sci.*, **37**, 1375 (1980).

the icing wind tunnel, were studied. By applying (1), a whole spectrum of values of n ranging from 0.01 to 0.3 was obtained.

It has been presently considered that new experiments on grain growth in ice should be performed to obtain a better evaluation of the parameters involved in the process and to recognize the possible dependence of the phenomenon on different sample features, such as the grain shape and the presence of air bubbles in the structure.

The application of the results to the interpretation of the structure of hailstones, collected in the ground and kept in some cases during a nonnegligible time in cold room before analysis, will also be considered.

2. – Experimental methods.

Polycrystalline ice cylinders were grown by the rapid freezing of double distilled water, inside a cylindrical brass container of 1 cm radius and 30 cm length, immersed in a cold liquid bath at $T \leqslant -24$ °C. The water was cooled down to 0 °C before pouring it into the cylinder and, in some cases, it was boiled previously in order to reduce the bubble content of the ice.

According to KNIGHT *et al.* ([7]) and PRODI and LEVI ([8]), the effects of the free ice surface on the grain growth process were avoided, by using as samples to be annealed thick cylindrical slices cut off the polycrystalline ice rods. Since the extremities of the latter were discarded due to their inhomogeneity, 4 or 5 pieces, about 4 cm thick, could be obtained from each cylinder.

All the operations performed on ice were done in a few hours after growth, keeping the samples at a temperature < -10 °C. The initial crystal structure of each thick sample was determined by analysing thin sections, cut off both its ends immediately before annealing. In this way, the homogeneity of the samples was also controlled and the minimum structural changes which could be correlated with annealing were evaluated. Usually the mean crystal dimensions could vary by less than 10 % along a cylinder.

Annealing at $T = 0$ °C was performed by placing the sample, packed in a sealed metal box, inside a thermostatized container. The annealing temperature, measured by a copper-constantan thermocouple, was maintained at the chosen value within ± 0.2 °C by means of an electronic control. Annealing at $T = 0$ °C was performed by immersing the ice sample, wrapped in a Parafilm foil, into an ice-water mixture.

The grain growth process was studied by analysing successive sections 0.5 to 1 mm thick cut off the annealed sample at the desired time.

In order to reveal the crystal structure of the samples, two successive layers of 2 % and 4 % solutions of Formvar in 1-2 dichloroethane were extended on their surface and they were allowed to dry under controlled conditions of humidity at a temperature of about -10 °C. As shown by previous authors

(see, for instance, AUDERMAUR *et al.* [9]), in this way the surface of the sample is first thermally etched and subsequently replicated by the plastic film. This may be finally analysed under the microscope to determine the grain size and orientation.

After obtaining each replica, the sections were reduced with the microtome down to about 300 to 400 μm thickness, and these thin sheets were viewed and photographed in natural light and between crossed polaroids, to reveal the general crystal structure and the air bubble content of the ice.

3. – Results.

3·1. *Structure of the just-grown cylinders.* – The main features of the crystallographic structure of the ice cylinders are shown in fig. 1 and 2. Figure 1 is a microphotograph of the thermally etched surface of a cylinder cross-section, replicated with the plastic Formvar film. The photograph shows the grain

Fig. 1. – Microphotograph of a replica, showing elongated grains (40 ×).

boundary grooves, limiting the crystals elongated in the radial direction, as well as the prismatic pits, which reveal the crystal orientation. It may be seen from the etch pit shape that, for most crystals, the *c*-axes are approximately normal to the grain elongation. Figure 2 is a photograph of a thin section of a cylinder, observed between crossed polaroids. The dark cross

(9) A. N. AUFDERMAUR, R. LIST, W. C. MAYES and M. R. DE QUERVAIN: *Z. Angew. Math. Phys.*, **14**, 574 (1963).

indicates that the crystal orientation shown in fig. 1 is a general characteristic of the whole structure.

In table I the initial mean crystal width $\overline{w}_0$ is given for several just-grown cylinders. This parameter was obtained from the replica analysis of the cross-section surfaces, by counting the grains intersecting a circumference of

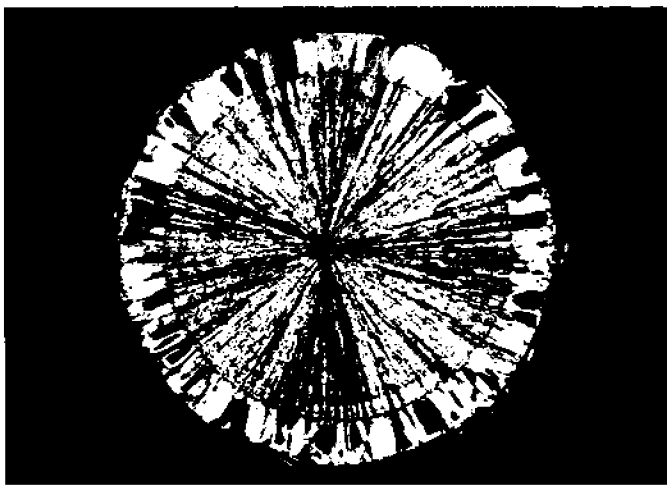

Fig. 2. – Thin section of a cylinder, observed between crossed polaroids.

5 mm radius. In this table, the temperature of the freezing bath used for each growth process is also indicated. It may be seen that $\overline{w}_0$ varied between 100 to 300 μm, with no strict relation to the freezing bath temperature. The mean grain length $\bar{l}_0$ was of the order of 1 mm. The mean grain size in the direction

TABLE I. – *Mean grain width and growth conditions for different cylinders.*

Cylinder No.	Initial mean crystal width $\overline{w}_0$ (mm)	Freezing bath temperature °C
4	0.27	−24
6	0.16	−24
17	0.08	−75
18	0.09	−27
19	0.25	−28

of the cylinder axis, measured in longitudinal sections of the cylinders, was found to be similar to $\overline{w}_0$.

For several samples, the frequency distributions of the maximum width w and the maximum length l were also obtained for about 200 crystals contained

in an annular zone of mean radius $r = 5$ mm. Examples corresponding to cylinder 6 are given in fig. 3. As shown in fig. 3*a*) and *b*), the initial w and l distributions were asymmetric with respect to their maximum and showed a tail on the side of large crystals. The w distribution, with its narrow peak and short tail, could be approximated by a log-normal curve. The maxima for both distributions of w and l differed only slightly from their mean values $\overline{w}$ and $\bar{l}$.

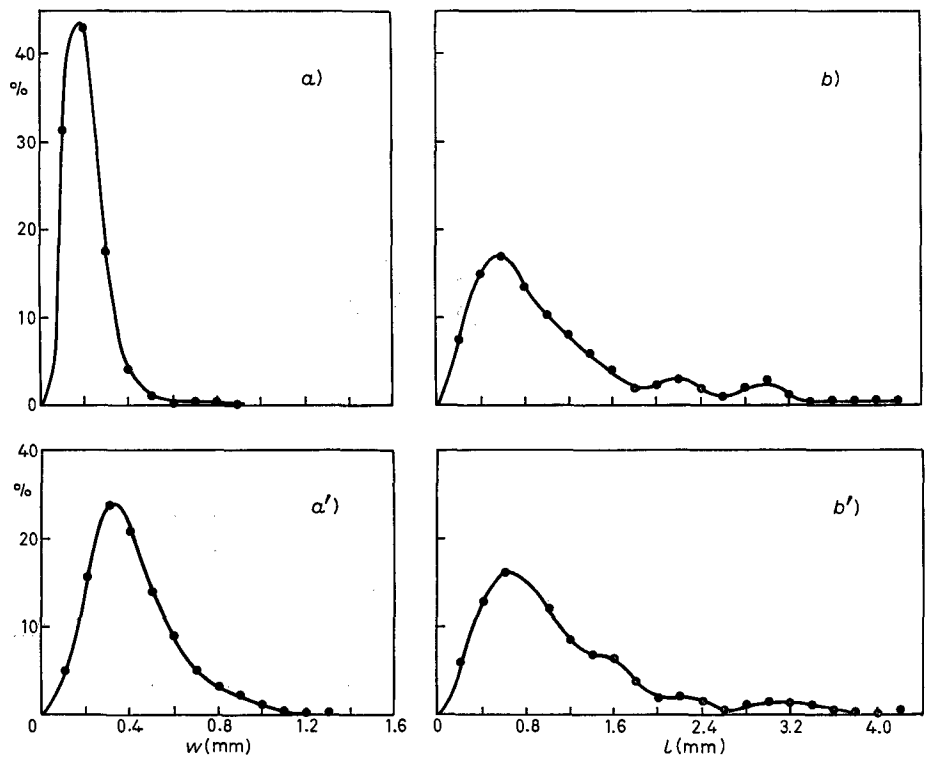

Fig. 3. – Distributions of w and l, in fresh and annealed samples (cylinder 6): *a*) w initial distribution, *b*) l initial distribution, *a'*) w distribution after 120 h annealing at -2 °C, *b'*) l distribution after 120 h annealing at -2 °C.

Air bubbles were present in all samples, though their concentration was slightly lower in cylinders 4 and 6, that were grown from boiled water. The initial aspect of very bubbly samples may be seen in fig. 4*a*), *b*) and 5*a*), *b*). The direct observation of thin sheets in natural light showed the presence of bubbles with diameters varying between 10 and 100 μm. The bubble size distributions could be observed to vary slightly from one sample to the other, though their detailed study could not be performed with the analysis methods used in the present work.

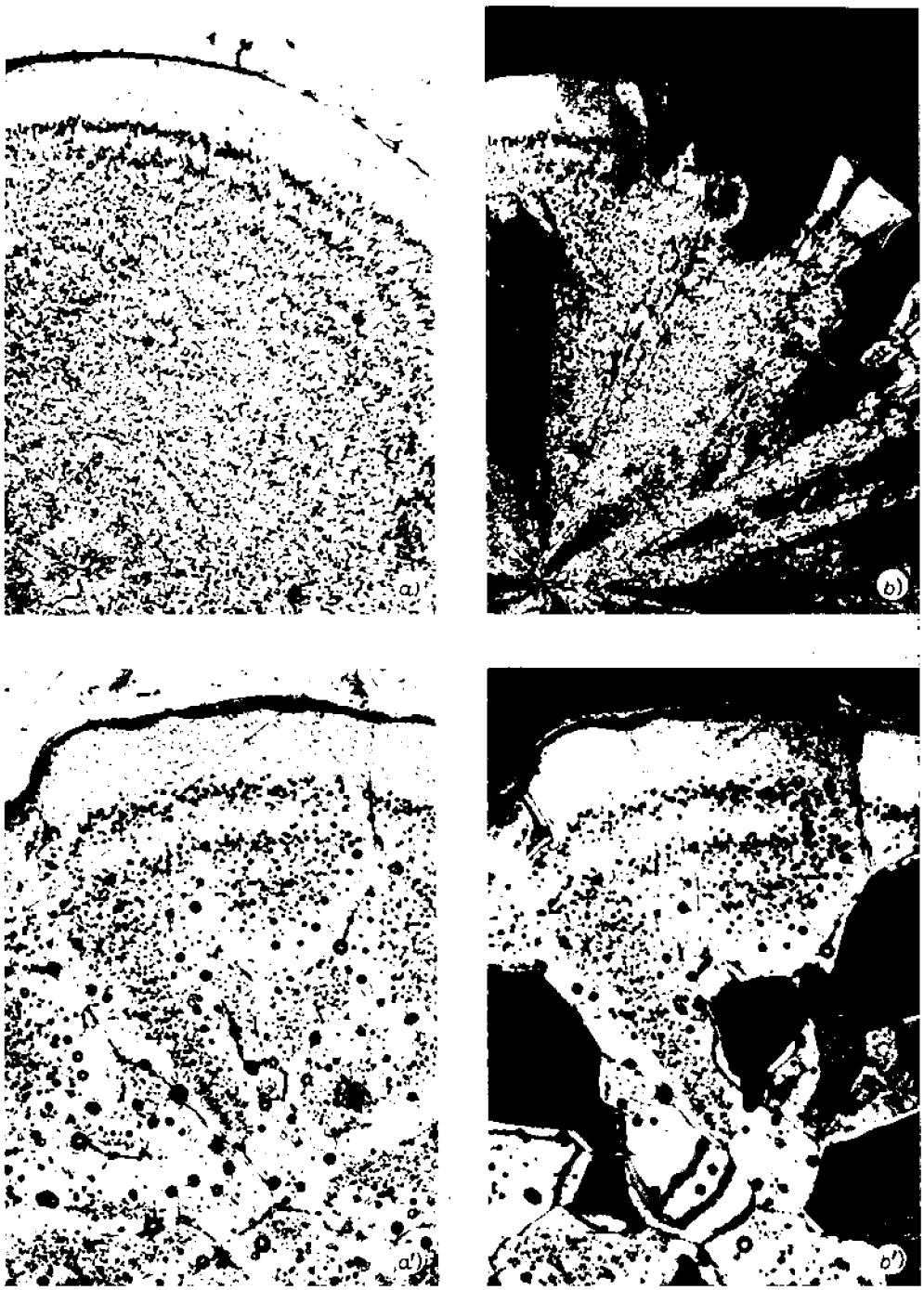

Fig. 4. – Photographs of thin cylinder sections showing the initial structure of a sample and the effects of annealing at $T = 0$ °C (cylinder 19): *a*) and *b*) thin sections cut off the just-grown cylinder observed in natural light and between crossed polaroids, *a'*) and *b'*) thin sections observed as in *a*) and *b*), but cut off a sample annealed 94 h at 0 °C.

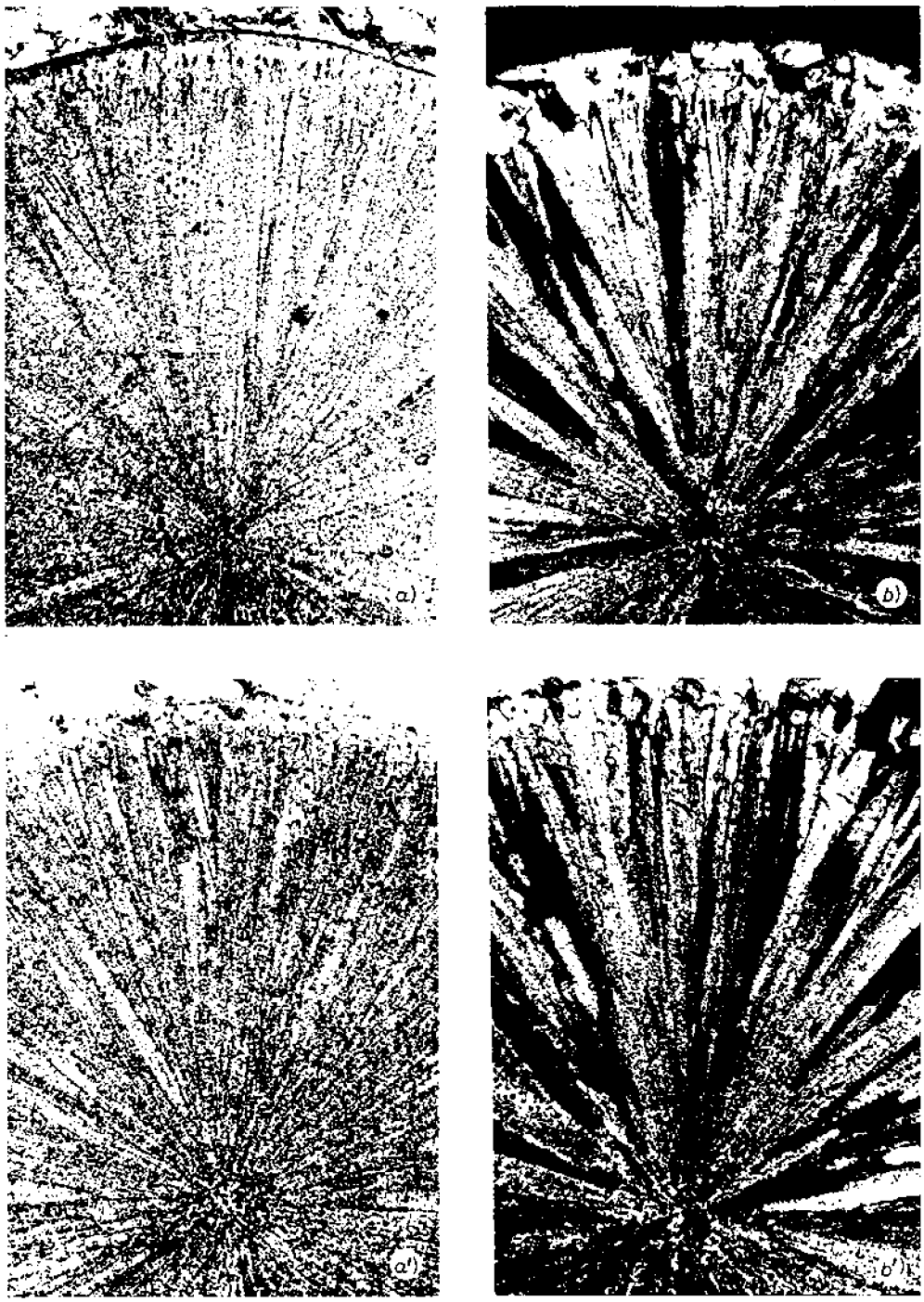

Fig. 5. – Photographs of thin cylinder sections showing the initial structure of a sample and the effects of annealing at $T = -2$ °C (cylinder 17): *a*) and *b*) as in fig. 4, *a'*) and *b'*) thin sections as in *a*) and *b*), but cut off a sample annealed 120 h at -2 °C.

3·2. *Changes of the sample structure due to annealing.* – The frequency distributions for w and l given in fig. 3*a'*) and *b'*) correspond to a section of cylinder 6, analysed 120 h after annealing at -2 °C. The comparison of fig. 3*a'*) with *a*) shows that the maximum of w is shifted to about twice its initial value, but that the width increase does not determine any fundamental modification of the corresponding frequency distribution; in fact, it may be easily verified that the curve in fig. 3*a'*) is still nearly log-normal and that both curves in fig. 3*a*) and *a'*) would approximately coincide if they were represented as functions of $w/w_m \simeq w/\overline{w}$, where w_m is the curve maximum. On the other hand, the comparison of fig. 3*b*), *b'*) shows that the l frequency distribution of the annealed sample practically coincides with the initial distribution, both for the location of the maximum and for the curve shape.

In general, the analysis of the annealed samples showed that in all cases the values of $\bar{l}$ and the shape of the corresponding frequency distributions were not modified by annealing while $\overline{w}$ increased with time. It was thus concluded that the radially elongated grains could be treated as cylindrical crystals with approximately constant length $\bar{l}$ and varying diameter $\overline{w}$, the curvature radius of the cylindrical boundaries being in this case $\frac{1}{2}\,\overline{w}$. The grain growth

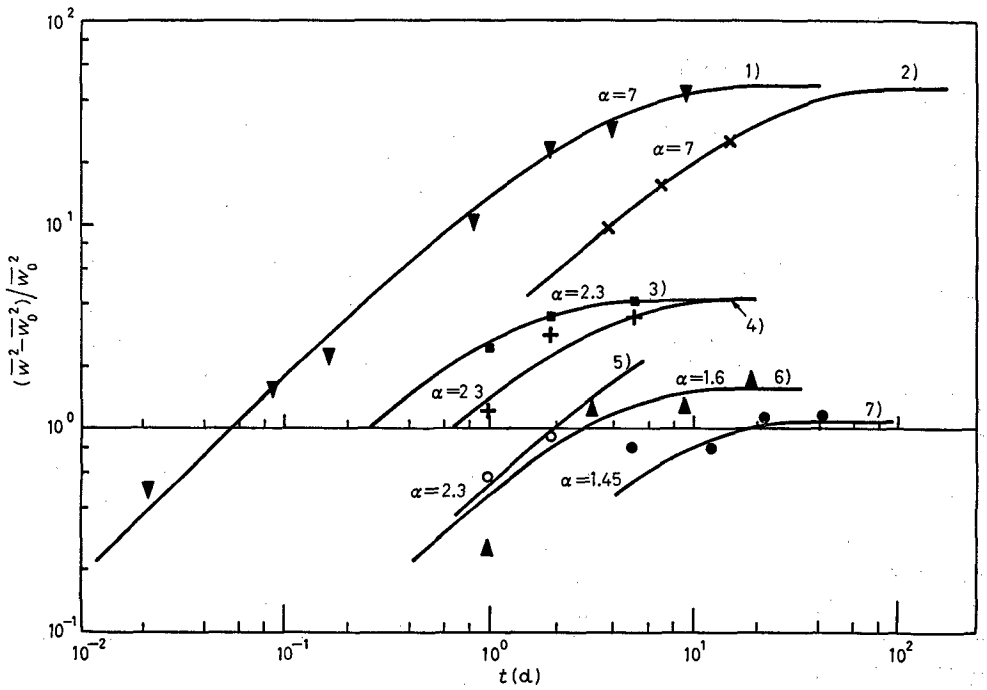

Fig. 6. – Annealing effects on $\overline{w}$: 1) annealing at $T = 0$ °C (cylinder 19), 2) annealing at $T = -0.5$ °C (cylinder 4), 3) annealing at $T = -2$ °C (cylinder 6), 4) annealing at $T = -6$ °C (cylinder 6), 5) annealing at $T = -11$ °C (cylinder 6), 6) annealing at $T = -2$ °C (cylinder 17), 7) annealing at $T = -6$ °C (cylinder 18).

process was consequently studied by determining $\overline{w}$ at successive annealing times t. The results have been represented in fig. 6, where $(\overline{w}^2 - \overline{w}_0^2)/\overline{w}_0^2$ is plotted as a function of t in a double-logarithmic scale. This representation takes into account that, when $\overline{w}_0$ is not negligible with respect to $\overline{w}$, one should write, instead of (1),

$$\overline{w}^m - \overline{w}_0^m = 2Kt, \tag{2}$$

where, according to the theory ([2-4]), it is $m = n^{-1} = 2$.

It may be seen in fig. 6 that the experimental points are not distributed along straight lines, as they should be if eq. (2) were valid. In general, the curve slope decreases with t, showing the tendency of $\overline{w}$ toward a limit value $\overline{w}_s$. The value of the ratio $\alpha = \overline{w}_s/\overline{w}_0$ is indicated on each curve. The meaning of this number will be discussed in the next section. The comparison of different curves in fig. 6 also shows that the grain growth rate, quite pronounced at or very near the melting point, decreases rapidly below this temperature.

For annealing temperatures $-2°$ C, -6 °C and -11 °C, two series of experiments were performed by using samples from cylinder 6, containing a relatively low air bubble concentration and from cylinders 17 and 18, formed by more opaque ice showing a large concentration of small bubbles. Notice that, for both groups of samples, the grain growth rate decreases with temperature, but that, at a given temperature, the phenomenon is slower for the samples of the second group, containing a larger bubble concentration. In the latter, the curve for -11 °C has not been presented in the figure, because, at this temperature, the grain growth rate was negligible from the beginning of the experiments.

On the other hand, the presence of air bubbles affected very slightly the grain growth process when the samples were annealed at or very near the melting point. In fact, the curve corresponding to cylinder 19, annealed at $T = 0$ °C, shows a rapid grain size evolution despite the bubble concentration being in this cylinder only slightly lower than in cylinder 17 (see fig. 4*a*), 5*a*)) and quite similar to that in cylinder 18.

The difference between the effects produced by annealing at the melting point and at a few degrees below this temperature, for samples containing a large bubble concentration, may be clearly seen in fig. 4 and 5. The comparison of fig. 4*a*), *a'*) and 4*b*), *b'*) shows that, after 94 h annealing at $T = 0$ °C, the grain width is markedly increased and the crystals appear less elongated in the radial direction. At the same time, the bubble distribution, approximately uniform in the just-grown sample, changes in the annealed one into a patched structure. Large bubbles clearly accumulate along grain boundaries, leaving bubble-free zones mostly at one side of the grain boundary grooves. On the other hand, the comparison of fig. 5*a*) and *a'*) shows that, even after 456 h annealing at $T = -2$ °C, *i.e.* very slightly below the melting point, a sample

initially containing a large bubble concentration does not show any appreciable change, both for the grain size and for the bubble distribution, by simple observation of a thin section in natural and polarized light.

4. – Discussion.

According to the classical theory of normal grain growth eqs. (1) and (2) with $m = 2$ and $n = \frac{1}{2}$ may be obtained by integration of the equation giving the grain growth rate:

$$\frac{\mathrm{d}\overline{w}}{\mathrm{d}t} = \varkappa \Delta F = K/\overline{w}\,, \tag{3}$$

where $\varkappa$ and K are factors that depend on T, and ΔF is the driving force for grain boundary migration. For normal grain growth in a pure material, ΔF is proportional to the grain boundary surface free energy σ and to the reciprocal of the grain surface mean curvature radius, in our case $\frac{1}{2}\overline{w}$, so that it is $K \propto \varkappa\sigma$.

Previous experimental results, mostly obtained by studying grain growth in metals ([10]), have shown, however, that (1) and (2) must be frequently applied with $m > 2$ and $n < \frac{1}{2}$. Several causes for this behaviour have been considered in several theoretical works ([11-14]). These are mainly the shape of the grain size frequency distributions, the sample texture and the presence of inclusions in the material.

In this section, the possible influence of these effects on the observed grain growth behaviour will be considered and the dependence of the factor K on the temperature will be subsequently discussed.

4·1. *Crystal size frequency distributions and crystal texture.* – The influence of the crystal size frequency distributions on the system evolution during annealing has been pointed out in different theoretical works on grain growth ([2,4,11-14]). According to the proposed grain growth models, expressions of the type (2) could only be applied when the frequency distributions of the crystal dimensions evolve in a quasi-stationary manner.

By considering now the results in sect. **3**, it may be noted that this condition was well enough satisfied for w. For instance, by applying the χ^2 test to the distributions in fig. 3*a*), *a'*), it was found that the probability for them to belong to a log-normal population was $\sim 5\,\%$ for the just-grown sample, while it was

([10]) C. J. SIMPSON, W. C. WINEGARD and K. T. AUST: *Grain Boundary Structure and Properties*, edited by G. A. CHADWICK and D. A. SMITH (London, 1976), p. 201.
([11]) V. YU. NOVIKOV: *Acta Metall.*, **26**, 1739 (1978).
([12]) V. YU. NOVIKOV: *Acta Metall.*, **27**, 1461 (1979).
([13]) O. HUNDERI, N. RYUM and H. WESTENGEN: *Acta Metall.*, **27**, 161 (1979).
([14]) O. HUNDERI and R. RYUM: *Acta Metall.*, **29**, 1737 (1981).

$\sim 50\,\%$ for the annealed one. This small variation does not seem to have affected in a measurable way the mean grain size evolution represented by $\overline{w}(t)$.

On the other hand, it should be noted that the presence of a strong texture in the studied samples could also be considered as a possible cause for the departure of $\overline{w}(t)$ from the normal grain growth behaviour, due to variations of the grain boundary free energy with the relative grain orientation. We have noted, however, that all the samples used in the present work were basically similar for their texture, though their annealing behaviour, as shown in fig. 6, could be quite different. Furthermore, the grain boundary interface free energy for ice is, according to previous results ([15]), nearly independent of the relative orientation. Only for exceptional cases, such as twins or adjacent crystals with approximately normal or parallel c-axes, this energy may be substantially smaller than its accepted value, of about 60 erg/cm^2. However, among these cases, only that of grains with nearly parallel c-axes could have been rarely present in the samples studied. In fact, the evidence that grains were not separated by low-energy grain boundaries was also shown by the deep grain boundary grooves always formed between adjacent grains on the surface.

It may be concluded that neither the evolution of the grain size frequency distributions nor the sample texture could have been the main cause of the difference between the curves in fig. 6 and those which should correspond to the theoretically expected grain growth behaviour.

4·2 *Effect of air bubbles on the grain growth behaviour.* – It has been noted ([10,14]) that, when particles of a second phase are present in a polycrystalline material, grain growth tends to stagnate, the mean crystal size approaching a limit value.

In order to account for this behaviour, the pinning action of inclusions has been introduced in the grain growth theory ([10,14]) by adding a retarding term (Zener drag) in the equations which represent the grain growth rate. Thus, if eqs. (2), (3) are used to represent the phenomenon in the pure material, according to BURKE ([15]) the effect of inclusions may be taken into account by writing

$$\frac{\mathrm{d}\overline{w}}{\mathrm{d}t} = \frac{K}{\overline{w}} - P = K\left[\frac{1}{\overline{w}} - \frac{1}{\overline{w}_s}\right], \tag{3'}$$

$$\frac{\overline{w}_0 - \overline{w}}{\overline{w}_s} + \ln\frac{\overline{w}_s - \overline{w}_0}{\overline{w}_s - \overline{w}} = \frac{K}{\overline{w}_s^2}t, \tag{2'}$$

where $P = K/\overline{w}_s$ is the retarding term and $\overline{w}_s$ is the limit diameter at which grain growth stagnates. According to BURKE ([15]), this is related to the mean diameter $\bar{d}$ of the inclusions and to their volume fraction f by the equation $\overline{w}_s = \bar{d}/f$.

([15]) J. E. BURKE: *Trans. Amer. Inst. Min. Metall. Pet. Eng.*, **180**, 73 (1949).

It may now be noted that, though the retarding term P has been originally introduced to take into account the effect of solid inclusions on the grain growth process, gas bubbles present in the matrix might play on this phenomenon quite a similar role.

This effect has been theoretically studied by SPEIGHT and GREENWOOD [16] for metals containing inert-gas bubbles, developed by irradiation. These authors noted that, while solid particles may be considered to remain in the matrix in a fixed position, gas bubbles may migrate by atomic or molecular diffusion occurring on their surface. Thus, when attained by an advancing boundary, they may be dragged due to the action of the boundary surface free energy. In this case, grain growth stagnation would not strictly occur, but the grain boundary velocity would decrease down to a limit value coinciding with that of the dragged bubbles. It may be concluded that, in the case of inclusions being gas bubbles, eqs. (3′) and (2′) would remain approximately valid, provided the considered limit velocity were much lower than the velocity of a free boundary.

Now, in order to interpret the present results, it has been assumed that the hindering effect of air bubbles on the boundary migration in ice crystals could be represented, as a first approximation, by eq. (2′). The curves corresponding to each series of experimental points in fig. 6 have consequently been obtained by assigning convenient values to $\overline{w}_s$, that is to the parameter $\alpha = \overline{w}_s/\overline{w}_0$ indicated on each curve. In this way also the parameter K has been evaluated. It may be observed that, while the value of α determines the shape of each curve, a variation of K only determines a shift of the whole curve in the direction of the horizontal axis.

The results obtained for K as a function of T will be discussed in subsect. 4·3. As for the parameter α, it may be interesting to relate its different values, varying from $\alpha = 7$ near the melting point to $\alpha \simeq 2$ at lower temperatures, to the bubble size and mobility in the ice crystals. Actually, though the present discussion should be considered as semi-quantitative, the equation $\overline{w}_s = \alpha\overline{w}_0 = \overline{d}/f$ may be used to obtain a theoretic evaluation of the bubble diameter $\overline{d}$, for given values of α and f. In the present case, f may be evaluated by taking into account that the air solubility in water, at the normal pressure, varies between $1.8 \cdot 10^{-2}$ and $2.9 \cdot 10^{-2}$ ml/cm^3 for $20\ ^\circ\text{C} \geqslant T \geqslant 1\ ^\circ\text{C}$ [17] and by assuming that this was the approximate volume of air changed into bubbles in the present ice samples. Thus, by considering the results obtained below the melting point, where $\alpha \simeq 2$, it is found, for $\overline{w}_0 = (200 \div 300)\ \mu\text{m}$, $\overline{d} = (10 \div 20)\ \mu\text{m}$. This is a reasonable value for the mean bubble diameter in the just-grown samples.

On the other hand, the value $\alpha = 7$ found very near the melting point may be related to different causes: 1) the increase, at this temperature, of the air

---

[16] V. M. SPEIGHT and G. W. GREENWOOD: *Philos. Mag.*, **9**, 683 (1964).

[17] J. N. CARRAS and W. C. MACKLIN: *Q. J. R. Meteorol. Soc.*, **101**, 127 (1975).

diffusivity in the matrix, that determines the increase of the mean diameter $\bar{d}$ during annealing, due to the growth of the larger bubbles at the expense of the smaller ones. In this case, the relatively large value obtained for α could be correlated with a bubble diameter $\bar{d} = (35 \div 70)$ μm, which is intermediate between that of the just-grown and of the annealed samples; 2) the increased mobility of air bubbles, which, at $T = 0$ °C, could be easily dragged by migrating grain boundaries. In this case, the grain boundary mobility would decrease with increasing annealing time mainly because of the formation of air layers in the boundaries, which would result in a reduction of the surface contact between grains. In these conditions the relation between α and $\bar{d}$ would not be strictly valid.

The features shown in fig. 4*a'*), *b'*) indicate that the latter mechanism operated. Actually air channels may be seen along boundary grooves, while some of the crystal zones nearly free of bubbles are asymmetric with respect to the corresponding grain boundary. This shows that the bubbles were probably swept away by the boundaries. In this case, the few large bubbles observed inside some of the grains could be assumed to have been left behind by boundaries that have disappeared due to shrinking of small grains.

4·3. *Activation energy.* – Grain growth is a thermally activated process, the activation energy being that of the grain boundary mobility. The parameter K in (3) or (3′) may be consequently written

$$K = K_0 \exp\left[-Q/RT\right]. \tag{4}$$

JELLINEK and GOUDA [1] considered that the constant factor Q_n in the exponent of (1′) could be treated as the activation energy for boundary migration, so that they identified the value obtained for Q_n with that to be introduced for Q into (4). Thus they discussed the phenomenon by assuming $Q \simeq Q_n = 5600$ cal/mol.

It must be noted, however, that according to eqs. (2) and (3) the exponent in (1) should be $n = \frac{1}{2}$, so that $k_n = K^{\frac{1}{2}}$ and $Q_n = \frac{1}{2}Q$. Now, since eq. (1) has been frequently applied with $n < \frac{1}{2}$, several authors have used the value Q_n/n to represent the activation energy for the grain growth process. In this case, Jellinek and Gouda's results would give $Q = Q_n/0.3 = 18.7$ kcal/mol.

However, it has recently been pointed out by SIMPSON *et al.* [10] that the activation energy for grain boundary migration may only be correctly derived by applying (1) if $n = \frac{1}{2}$. For $n < \frac{1}{2}$, the equation to be used would be eq. (2), when $m = 2$ for a convenient value of $\bar{w}_0 \neq 0$. When this condition is not satisfied and retarding effects on the boundary migration must be taken into account, an equation of type (2′) should be used, as indicated in **4·2**.

Now, in order to compare the results of Jellinek and Gouda with the present ones, eq. (2′) has also been applied to the former, whereby $\bar{w}_0$ at $t = 0$ was made to coincide with the first point of each series of experiments. It was

found that, in this case, the experimental points could be satisfactorily represented by (2′) with $\alpha \simeq 3$. Thus new values of K were calculated. The latter values and those resulting from the curves in fig. 6 are plotted in fig. 7 *vs.* T^{-1}. From the straight line drawn through the points obtained from Jellinek and Gouda's data and from the present results corresponding to the $\alpha > 2$ curves, it is derived $K_0 = 1.4 \cdot 10^5$ mm^2 s^{-1}, $Q = 13.4$ kcal/mol $= 0.58$ eV.

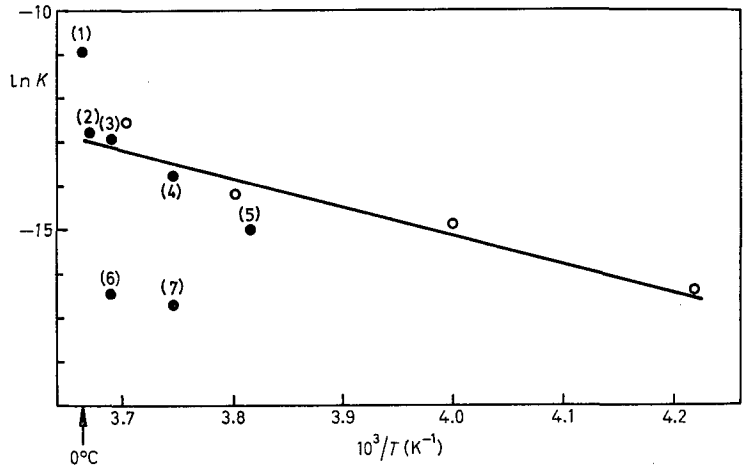

Fig. 7. – ln K as a function of T^{-1}; K is given in mm^2 s^{-1}. o points derived from JELLINEK and GOUDA, • present results, these are labelled by the cylinder number.

The points of the K diagram from the $\alpha < 2$ curves in fig. 6 are found below the considered line, but this may be explained by observing that the error in the evaluation of K may be large when the curves in fig. 6 are, from the beginning, at a small angle to the horizontal axis. On the contrary, the point corresponding to $T = 0$ °C is found slightly above the straight line, probably because the phenomenon is modified by the beginning of melting.

It may be interesting to observe that the obtained value of Q approximately coincides with that of bulk self-diffusion in ice, $Q = 0.60$ eV $=$ $= 13.8$ kcal/mol ([18]). This coincidence is in agreement with previous results obtained for metals ([10]) and it has been theoretically explained by assuming that the boundary migration is controlled by the bulk diffusion of impurities in the lattice. It should be noted, however, that, in the case of metals, the curves giving the logarithm of the grain boundary mobility *vs.* T^{-1} present a sharp decrease of slope when the temperature increases above a transition value. At this transition the activation energy would change from that of bulk self-diffusion to that of boundary self-diffusion. It has also been found that, for a given material, the temperature of the transition is higher for a lower

([18]) P. V. HOBBS: *Ice Physics* (Oxford, 1974).

driving force and it is located a few degrees below the melting point in the case of normal grain growth. This behaviour has been interpreted by assuming that, for a given driving force, the grain boundary migration would become, at a certain temperature, independent of the surrounding impurity atmosphere, changing to a process controlled by jumps of atoms or molecules in the boundary.

Now, the constant value of Q obtained here for ice, on the basis of the present and of Jellinek and Gouda's results, indicates that the mechanism of impurity bulk diffusion would control the phenomenon in the whole temperature range, going from -30 °C to 0 °C. The lack of the transition to a lower value of the activation energy could be explained by taking into account that the boundary surface free energy is for ice about two orders of magnitude lower than that found for metals. It is consequently possible that the driving force operating in grain growth would be in the case of ice so low that, even for the small concentration of impurities present in ice grown from distilled water, the boundary migration would be controlled by bulk diffusion of these impurities up to the very melting point.

5. – Conclusions.

As a summary of the results described in sect. **3** and of the discussion in sect. **4**, the following points may be considered:

1) When grains forming a polycrystalline sample are initially elongated, their mean length may remain practically unchanged during annealing, while their mean width increases according to laws (2) or (2′). Accordingly, the shape factor $\bar{\varepsilon} = \bar{l}/\bar{w}$ decreases while the crystals tend to an isotropic shape. Thus, when crystals are elongated, the grain growth theory may not be applied, as usual, to the mean crystal dimensions, $\sqrt{\bar{a}}$, where $\bar{a}$ is the mean crystal area, but to the mean crystal width $\bar{w}$. This result agrees with previous ones for elongated crystals forming accretions ([7,8]). It has been noted that, in accreted ice, the crystal length may even decrease with time. The fact that this latter behaviour has not been observed in the present samples could be possibly related to some difference in the shape of grains, which, in the case of accreted ice, are not only elongated but also limited by irregular boundaries.

2) The effect of air bubbles on the grain boundary mobility in ice has not been previously studied in some detail. According to the present results, this effect would be strong below the melting point. Thus, since even slightly opaque ice contains a large number of small air bubbles, grain growth in most accreted ice would be hindered after a few hours annealing at $T < 0$ °C.

3) The hindering effect of air bubbles on the grain growth process would be highly reduced at the melting point. This may be due to the rapid increase of the air bubble diameter and mobility occurring when melting is approached.

This result agrees with the observation of Roos ([6]), who found that, for T varying between 0 °C and — 1 °C, bubbles have no effect on the grain growth rate. It also explains previous results obtained by KNIGHT *et al.* ([7]) who, studying accreted ice, observed rapid structural changes at $T = 0$ °C.

4) These results may be important for applications to the study of hailstones. Actually, the presence of air bubbles should be taken into account when the structure of their different layers is interpreted. Due to grain growth stagnation, opaque layers of hailstones stored at the usual cold room temperature would slightly change their structure. Important grain growth effects could occur, however, during the short stages of the samples at $T = 0$ °C, which could have occurred before collection. Thanks to the very slow grain growth at $T < 0$ °C, grains with dimensions < 500 μm are frequently found in opaque layers, even after several months of storage in cold room.

5) The value of the grain growth activation energy found in the present work, $Q = 0.58$ eV, is reasonable because it coincides with the activation energy for bulk self-diffusion. This value indicates that, even when ice is obtained from distilled water, grain growth is controlled by bulk impurity diffusion.

* * *

The authors are thankful to O. NASELLO for useful contributions to this work. The CONICET is acknowledged for financial support.

● RIASSUNTO

Si studia l'accrescimento di grano in ghiaccio policristallino, formato di grani allungati, con spessore medio $\overline{w}$ di (200÷300) μm e lunghezza media $\bar{l}$ di (2÷3) mm. I campioni si fanno ricuocere a diverse temperature, fra 0 °C e — 10 °C. Si osserva che $\bar{l}$ non è modificata dalla ricottura mentre $\overline{w}$ cresce col tempo del trattamento. Al di sotto del punto di fusione, $\overline{w}(t)$ tende a un valore limite $\overline{w}_s$. Questo comportamento si mette in relazione con l'azione inchiodante delle bolle d'aria, che si considera simile a quella attribuita a inclusioni solide in metalli. Supponendo $\overline{w}_s = \bar{d}/f$, dove $\bar{d}$ è il diametro medio delle bolle e f è la frazione di volume dell'aria dissolta nell'acqua, si ottengono valori ragionevoli per $\bar{d}$. Si valuta l'energia d'attivazione del fenomeno, sulla base dei risultati attuali e di quelli di Jellinek e Gouda. Il valore ottenuto, $Q = 0.6$ eV, coincide approssimativamente con quello di autodiffusione di volume, come succede per i metalli, a temperature di vari gradi inferiori al punto di fusione. Questa coincidenza suggerisce che, per il ghiaccio, l'accrescimento di grano sarebbe controllato dalla diffusione di volume d'impurità, praticamente fino al punto di fusione.

Резюме не получено.